Electronic Supplementary Material (ESI) for RSC Advances.

Synthesis of Silanized Magnetic Ru/Fe_3O_4@SiO_2 Nanospheres and its High Selectivity to Prepare *Cis*-pinane

Yue Liu [a], Lu Li [b], Shiwei Liu [b], Congxia Xie [a] Shitao Yu [b,*]

[a] *Key Laboratory of Sensor Analysis of Tumor Marker Ministry of Education, College of Chemistry and Molecular Engineering, Qingdao University of Science and Technology, 53 Zhengzhou Road, Qingdao 266042, Peoples Republic of China*

[b] *College of Chemical Engineering, Qingdao University of Science and Technology, 53 Zhengzhou Road, Qingdao 266042, Peoples Republic of China*

CONTENTS

S1. Details of FT-IR Spectra

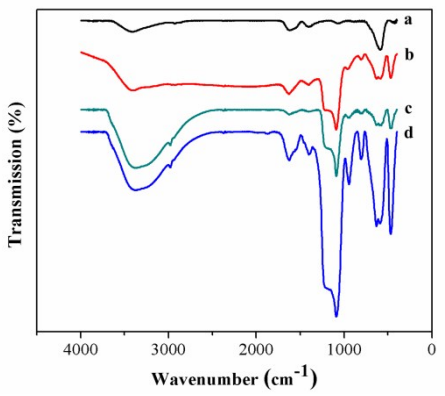

Fig. S1 FT-IR spectra of (a) Fe_3O_4, (b) Fe_3O_4@SiO_2, (c) Fe_3O_4@SiO_2/APTS/Ru, (d) Fe_3O_4@SiO_2/MPTS/Ru.

Fig. S1 shows FT-IR spectra of the as-prepared magnetic particles. The absorption band at 586 cm^{-1} in curve **a** is ascribed to Fe–O–Fe vibrations, which also confirms the magnetic particles are Fe_3O_4 [1, 2]. In comparison with curve a, the sharp peak at 1,086 cm^{-1} in curve b can be assigned to the Si–O–Si vibrations, whereas the peaks around 1,629 and 3,432 cm^{-1} are attributed to the absorbed water and hydroxy groups [3]. The Si–O bending vibration mode of the silanol group is seen at 959 cm^{-1}. After modification with APTS (curve c), the peaks detected at 2,960 cm^{-1} can be assigned to the C–H bonds from the silane APTS, Contributions from $–NH_2$ group were probably overlapped by vibration bands related with silanol groups and adsorbed water [4, 5]. After modification with MPTS (curve d), the peak at 671 cm^{-1} is attributed to the C–S bending vibration mode [6]. The peak at near 2570–2590 cm^{-1} is attributed to the stretching vibration mode of S–H. The S–H stretching vibration mode is not usually detected [7]. However, the band at around 2850–2960 cm^{-1} is due to the stretching vibration of C–H of methylene. This result suggests that the surface modification of Fe_3O_4@SiO_2 core–shell nanospheres was successful prepared.

S2 TEM and particle distributions of Ru/Fe_3O_4@SiO_2

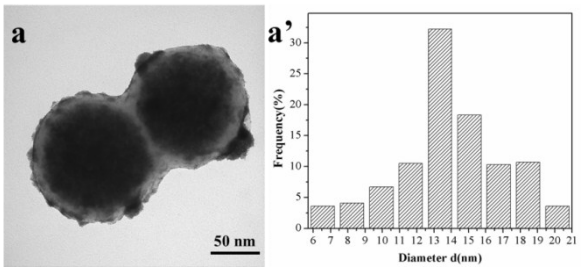

Fig. S2 TEM and particle distributions of $Ru/Fe_3O_4@SiO_2$ (a and a').

S3 The magnetic separation process of $Fe_3O_4@SiO_2$/APTS/Ru microspheres

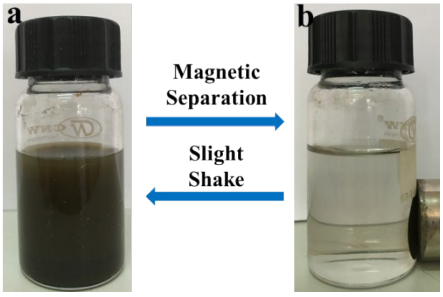

Fig. S3 Photograph of the catalyst dispersed in reaction mixture (a) and magnetic separation of the catalysts from the reaction medium (b).

S4 Details of magnetization curves

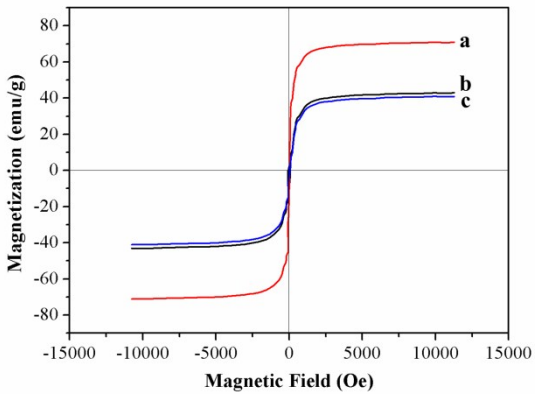

Fig. S4 Magnetization curves of Fe_3O_4 (a), $Fe_3O_4@SiO_2$ (b) and $Fe_3O_4@SiO_2$/APTS/Ru (c).

The magnetic properties of Fe_3O_4, $Fe_3O_4@SiO_2$, and $Fe_3O_4@SiO_2$/APTS/Ru nanoparticles were investigated using a vibrating sample magnetometer. Results are shown in Fig. S4. All samples showed hysteresis loops without any detectable remanence, reflecting the superparamagnetic properties of the samples. The magnetization saturation values of $Fe_3O_4@SiO_2$, and $Fe_3O_4@SiO_2$/APTS/Ru were 43.6

emu g^{-1} and 41.1 emu g^{-1}, respectively. The decrease of the saturation magnetization suggests the presence of some Ru particles on the surface of the magnetic supports. Even with this reduction in the saturation magnetization, the catalyst was still efficiently and easily separated from the solution with the help of an external magnetic force. As a result of the superparamagnetic properties and high magnetization, the Fe_3O_4@SiO_2/APTS/Ru nanoparticles showed fast separation under the applied magnetic field and quick dispersion through a slight shake when the magnetic field was removed.

S5 The reusability of Fe_3O_4@SiO_2/MPTS/Ru

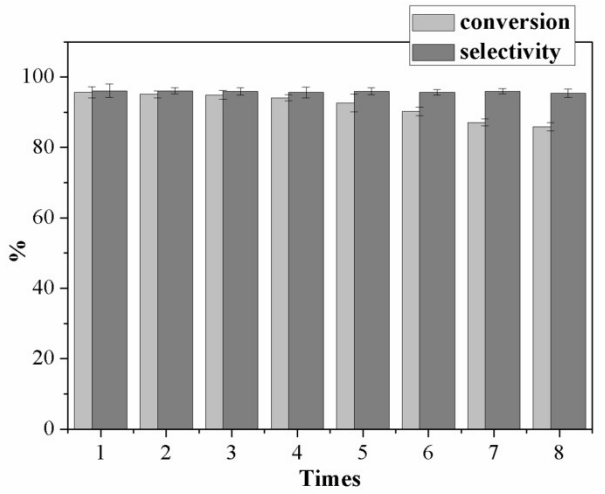

Fig. S5 The reusability of Fe_3O_4@SiO_2/MPTS/Ru. Reaction conditions: α-pinene 2.72 g, Fe_3O_4@SiO_2/MPTS/Ru 0.13 g (the thicknesses of the silica layer were about 25.6 nm, Ru 10 wt%), H_2 4 MPa, 120°C, 4 h.

S6 Details of XRD patterns

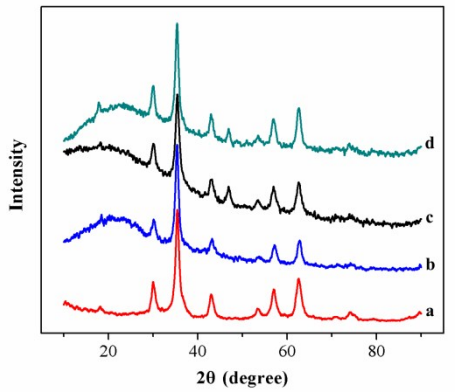

Fig. S6 XRD patterns of Fe_3O_4 (a), Fe_3O_4@SiO_2 (b), Fe_3O_4@SiO_2/APTS/Ru (c) and Fe_3O_4@SiO_2/MPTS/Ru(d).

The crystallinity and phase composition of the resulting products were investigated by X-ray powder diffraction (XRD). Fig. S6 exhibited the wide angle XRD patterns of the samples. As shown in Fig. S6a, all the peaks were in agreement with a face centered cubic structure of Fe_3O_4. After coating by SiO_2, a new broad peak around 23° appeared because of the existence of amorphous silica. For the Fe_3O_4@SiO_2/APTS/Ru and Fe_3O_4@SiO_2/MPTS/Ru samples, in addition to the Fe_3O_4 diffraction peaks, a tiny peak at 44° was distinguishable, which was owed to the characteristic diffraction peaks of Ru(0). The XRD results indicated that the Ru nanoparticles had been successfully loaded onto the surface of the Fe_3O_4@SiO_2/APTS and Fe_3O_4@SiO_2/MPTS microspheres. The average size of crystallite, calculated using Scherrer's equation, was about 2.5 and 4.0 nm, well in agreement with the average particle size derived from TEM analysis [8].

S7 Details of TGA curve

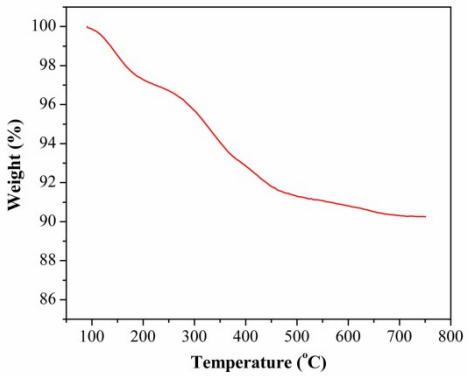

Fig. S7 TGA curve of Fe_3O_4@SiO_2/APTS/Ru.

Typical TGA curves of samples under a N_2 atmosphere are depicted in **Fig S7**. As can be seen from the diagram, Fe_3O_4@SiO_2/APTS/Ru was relatively stable around or below 300°C. The weight loss (3.02 wt%) at temperatures below 180°C can be attributed to water thermo-desorption from the surface of the silica layer, while weight loss above 500°C is associated with the release of hydroxyl ions from the particles. As shown in **Fig S7** the observed large weight reduction in the TGA curve of Fe_3O_4@SiO_2/APTS/Ru shows a weight loss (3.11 wt%) from 300 to 500°C apart from the three other loss events, which can be mainly resulted from the decomposition of aminopropyl groups introduced in functionalized magnetic nanoparticles [9].

Reference

[1] S. K. Li, F. Z. Huang, Y. Wang, Y. H. Shen, L. G. Qiu, A. J. Xie and S. J. Xu, *J. Mater. Chem.*, 2011, 21, 7459.

[2] S. Xuan, L. Hao, W. Jiang, X. Gong, Y. Hua and Z. Chen, *J. Magn. Magn. Mater.*, 2007, 308, 210.

[3] M. Shao, F. Ning, J. Zhao, M. Wei, D. G. Evans and X. Duan, *J. Am. Chem. Soc*., 2011, 134, 1071.

[4] Y. Deng, Y. Cai, Z. Sun, J. Liu, C. Liu, J. Wei, W. Li, C. Liu, Y. Wang and D. Zhao, *J. Am. Chem. Soc.*, 2010, 132, 8466.

[5] S. K. Li, X. Guo, Y. Wang, F. Z. Huang, Y. H. Shen, X. M. Wang and A. J. Xie, *Dalton. Tont.*, 2011, 40, 6745.

[6] D. V. Quang, J. E. Lee, J. K. Kim, Y. N. Kim, G. N. Shao and H. T. Kim, *Powder Technol*., 2013, 235, 221.

[7] S. Zhang, Y. Zhang, J. Liu, Q. Xu, H. Xiao, X. Wang, H. Xu and J. Zhou, *Chem. Eng. J.*, 2013, 226, 30.

[8] L. Zhou, C. Gao and W. Xu, *Langmuir*, 2010, 26, 11217.

[9] J. Zhang, S. Zhai, B. Zhai, Q. An and G. Tian, *J Sol-Gel Sci Technol*., 2012, 64, 347.